The Order Parameter of the Liquid-Liquid Transition in a Molecular Liquid – Supplementary Information

Joanna Mosses, Christopher D. Syme, and Klaas Wynne
School of Chemistry, WestCHEM, University of Glasgow, Glasgow, G12 8QQ, UK

Methods

Materials

Experiments were carried out on triphenyl phosphite TPP using the dyes coumarin 153 (C153) and perylene (FIG. 1), which were purchased from Sigma Aldrich and used as supplied. For the fluorescence microscopy experiments, the concentration of all solutions was ~10^{-5} M. At concentrations up to 10^{-4} M, we can experimentally rule out aggregation of the dye molecules used in TPP. For all microscopy experiments, a sample thickness of 11.58 ± 0.19 μm was used controlled by glass monodisperse particle standards (Whitehouse Scientific). Temperature was controlled to ± 0.1 K using a Linkam THMS600 microscope stage and T95 controller. In the experiments, the samples were quenched and held at a selected temperature.

Some of the experiments required the formation of the thermodynamically stable crystalline state (crystal 1). Crystal 1 was prepared by rapid supercooling of liquid 1 to about 230 K following by slow heating to about 280 K. The temperature was then lowered to a desired value and measurements performed.

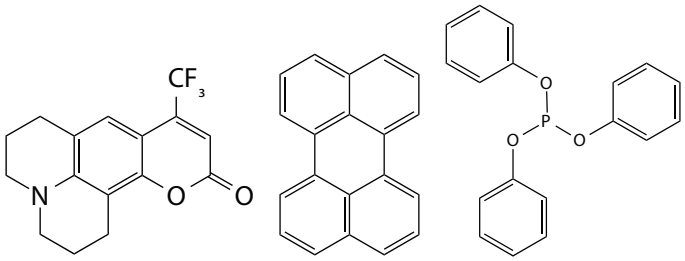

FIG. 1. The structure of Coumarin 153 (C153, left), perylene (center), and triphenyl phosphite (right).

Microscopy

Microscopy experiments were performed using a Zeiss LSM710 laser-scanning confocal microscope equipped with a 20× objective lens (NA = 0.4) providing a spatial resolution of 0.4 μm. Areas of ~212.1 × 212.1 μm^2 were mapped with a total acquisition time of ~30 s per frame. This system could be used for differential interference contrast (DIC), phase-contrast, and fluorescence microscopy using a number of CW laser sources ranging from 405 nm to 633 nm. For FLIM measurements, the system used a 405-nm laser pulsed at 20 MHz and a Becker & Hickl Simple-Tau detection system for time-correlated single photon counting (TCSPC).

Data acquisition

FLIM images comprising 256 × 256 pixels were obtained at an approximate average photon flux of ~1×10^6 photons s^{-1}, and data were accumulated such that the total photon count was sufficient for fitting purposes (at approximately 3,500 photons per pixel followed by 9-pixel binning, which is applied as a sliding average). Fluorescence decay curves were collected to a total delay time of ~50 ns to ensure a good fit (χ^2 ~1) and an accurate determination of the background noise level in order to avoid underestimating the lifetime.

Data analysis

Data analysis was performed using SPCImage software (Becker & Hickl). To obtain the fluorescence lifetime distributions, the accumulated fluorescence decay curves in each pixel of the scanned area were fitted with an appropriate model; in all of our measurements this model was a single exponential decay yielding a lifetime for each pixel in the image. As the measured fluorescence lifetimes were much longer than the instrument response function (IRF) of the FLIM system, tail fitting was applied to all decay curves. To check the accuracy of the tail-fitting method, a number of full fits (starting from the rise of the decay curve and including an experimentally obtained IRF) were performed and yielded the same lifetime values within the signal-to-noise ratio. For the data shown here, tail fits were carried out from 2 ns after the peak of the fluorescence decay curve (where the IRF has fallen to 1/1000th of its peak value) to about 30 ns where the fluorescence had decayed to the noise level. The fluorescence lifetime distributions so obtained where fitted to one or two Gaussians (see FIG. 2). It was verified that the 9-pixel binning procedure did not affect the lifetime distributions apart from a reduction in width by a factor of $\sqrt{9}$.

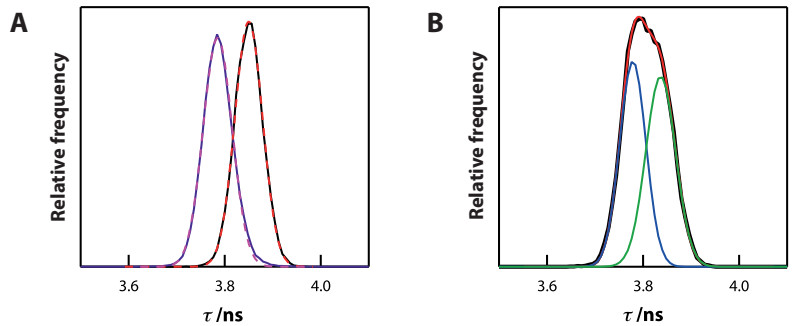

FIG. 2. The fluorescence lifetime distributions and corresponding gaussian fits of perylene in TPP at 220 K. (A) The lifetime distribution of liquid 1 (right/black) and liquid 2 (left/purple) and the corresponding single gaussian fits (dashed lines). (B) The lifetime distribution obtained at the stage when the sample in the scan area contained liquid 1 and liquid 2 in about 1:1 ratio. This distribution was fitted with two gaussian profiles.

Solvation

The dye molecule Coumarin 153 (C153) is commonly used to measure time-dependent solvation by use of the dynamic fluorescence Stokes shift measurement technique.[1-5] However, TPP in the range of temperatures studied here is extremely viscous (from 3.74×10^6 cP at 220 K to 8.57×10^6 cP at 213 K[6]) and the solvent relaxation time is therefore much longer than the excited-state lifetime of the dye. Hence, fluorescence will take place from an excited state in which the solvent has not relaxed, that is, where the solvent has not adjusted to the new excited-state dipole moment of C153 (FIG. 3). A certain degree of intramolecular vibrational relaxation can still take place, giving rise to a small (and fixed on the fluoresce timescale) Stokes shift.

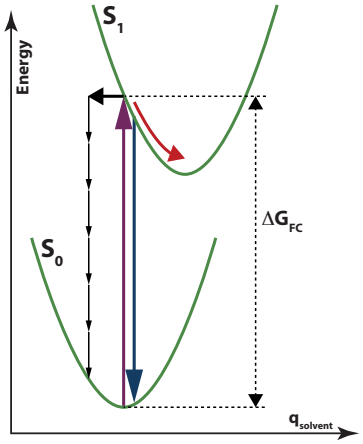

FIG. 3. Relaxation of the dye molecule C153 after excitation in the first electronically excited state. The permanent electric dipole moment of C153 is different in the ground and first electronically excited state. Normally, the solvent would relax around the dipole of the excited state. However, the extremely long solvent relaxation times in supercooled TPP prevent solvent relaxation within the excited-state lifetime. Thus, internal conversion will take place from the unrelaxed excited state.

The samples are prepared above the melting temperature of TPP, where solvent relaxation is fast (sub-picosecond). Thus, the solvent will adjust to the ground-state dipole moment of the C153 molecules before the samples are cooled and the LLT takes place on a typical transformation timescale of hours. Changes in the static dielectric constant (changes in the polarity) will affect the electronic energy gap in C153 through solvation. The absorption energy in the Franck-Condon region is then given by:[7-8]

$$\Delta G_{FC} = \Delta U^0 + \tfrac{1}{2}B_S\left(\mu_g{}^2 - \mu_e{}^2\right) + \tfrac{1}{2}B_{or}\left(\mu_g - \mu_e\right)^2, \qquad (1)$$

where ΔU^0 is the Franck-Condon absorption energy in vacuum, μ_g is the permanent dipole moment of the dye molecule in the ground state, μ_e that in the excited state, and in the Onsager cavity description:[7-9]

$$B_\infty = \frac{2}{4\pi\varepsilon_0 r^3}\frac{\varepsilon_\infty - 1}{2\varepsilon_\infty + 1}, B_S = \frac{2}{4\pi\varepsilon_0 r^3}\frac{\varepsilon_s - 1}{2\varepsilon_s + 1}, B_{or} = B_S - B_\infty, \quad (2)$$

where ε_0 is the permittivity of vacuum, ε_S the static dielectric constant, ε_∞ the infinite frequency dielectric constant, and r the radius of the Onsager cavity. For C153, μ_g = 6.6 D, $\mu_e \approx$ 11 D,[10] and the Onsager cavity radius is estimated at r = 3.2 Å. For the infinite frequency dielectric constant one can either use the value of 3.4 measured previously[11] or use the visible light refractive index $(1.59)^2 = 2.5$, with very little difference in the final outcome. The static dielectric constant measured previously[11] in liquid 1 of TPP is $\varepsilon_{S,liquid1} = 4.73$. However, the static dielectric constant reported for liquid 2 is unreliable because of the extremely long (~100 s) relaxation times. Therefore, it is assumed that the value for liquid 2 is relatively close to that of liquid 1. FIG. 4 shows the calculated change in the absorption energy in the Franck-Condon region in C153.

The radiative lifetime of C153 is 5.3 ns[12] but the observed lifetime is the inverse of the sum of the radiative rate and the rate of internal conversion. The rate of internal conversion is given approximately by the Jortner-Bixon expression[8, 13]

$$k_{JB} = \frac{2\pi V^2}{\hbar\sqrt{4\pi\lambda_S k_B T}} e^{-S} \sum_{n=0}^{\infty} \frac{S^n}{n!} \exp\left\{-\left(\Delta G^0 - \lambda_S - n\hbar\omega\right)^2 / \left(4\lambda_S k_B T\right)\right\}, \quad (3)$$

where V is the internal-conversion coupling constant, λ_S is the solvent reorganization energy, ΔG° is the energy gap, ω is the angular frequency of a high-frequency accepting mode, S is the Huang-Rhys factor, and the sum runs over n quanta of this high frequency mode.

In previous temperature-dependent fluorescence-lifetime experiments on C153,[14-15] it had to be taken into account that the fluorescence transition-dipole moment was changing with temperature. This is on account of the spectral shift in the fluorescence spectrum, which causes the transition dipole moment to change in proportion to

$$\frac{\int I(\nu)d\nu}{\int I(\nu)\nu^{-3}d\nu}. \quad (4)$$

In the temperature range used here, solvent relaxation in TPP is negligible on the fluorescence timescale and hence the Stokes shift is negligible. Therefore this effect does not have to be taken into account.

To calculate a reasonable non-radiative decay rate, we have set the coupling constant to 30 cm^{-1}, S = 0.85, and the frequency of the accepting mode to 2800 cm^{-1} corresponding to a typical CH-stretch vibrational mode. The solvent reorganization energy has been set to 3000 cm^{-1} and is considered to include the many (otherwise unaccounted for) lower frequency intramolecular modes as well as β relaxation of the solvent (TPP). The excited-state lifetime (accounting for radiative and non-radiative decay) is shown in FIG. 4 as a function of the dielectric constant of the medium (and the energy gap calculated using Eq. (1)). It can be seen that the excited state lifetimes are in good agreement with the measured values for C153 in TPP for dielectric constants in the range 3 to 5. Although the precise results depend on the parameters used, it is safe to state that the excited state lifetime scales linearly with the solvent polarity as expressed by the dielectric constant for the experimental parameters relevant to our experiments.

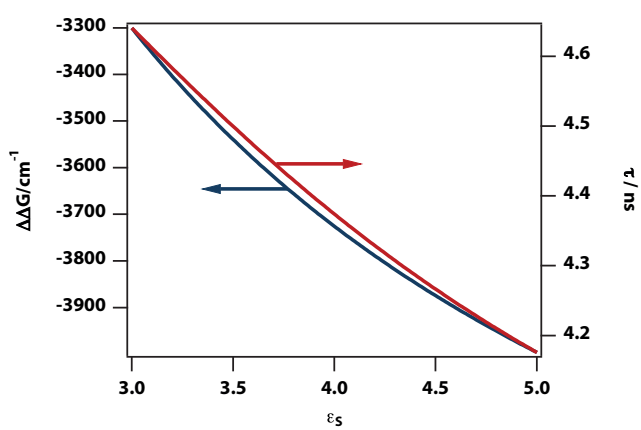

FIG. 4. Effect of solvent polarity on the energy gap and excited-state lifetime. Shown in blue is the calculated effect of solvation on the absorption and unrelaxed fluorescence energy gap in C153 based on Eq. (1) for a range of solvent dielectric constants. In red, the excited-state lifetime (accounting for radiative and non-radiative decay) predicted for C153 based on Eq. (3).

FLIM *vs.* TCSPC

FLIM measurements can resolve small differences in decay times in an inhomogeneous sample that cannot be resolved by bulk measurements. To demonstrate this, we have simulated TCSPC data using an exponential decay function that incorporates Poisson noise (simulating the effect of laser noise) decaying to a Poisson noise floor (simulating the effect of detector noise). The simulated TCSPC data removes ambiguities due to pulse shape in the experimental data.

FIG. 5 (top right) demonstrates that if two separate regions are measured with decay times of 4.0 and 4.3 ns, fitting the data can easily resolve these decays. When these two data sets are summed into a single set to simulate a bulk measurement, fitting the data with a single exponential (see FIG. 5 (bottom right)) gives an average decay time of 4.15 ns and a χ^2 close to 1. Fitting to a double exponential does not improve the fit and does not allow the extraction of the two decay times. The same effect is seen in the actual data: we can easily discern the decay times in liquid 1 and liquid 2 using FLIM. However, when all the TCSPC data from an image is averaged into a single TCSPC decay curve, the decay appears single exponential with a decay time that is the average of that in liquid 1 and liquid 2. Thus, FLIM is the only method known to discern small inhomogeneities in lifetimes and is therefore critical to the study presented here.

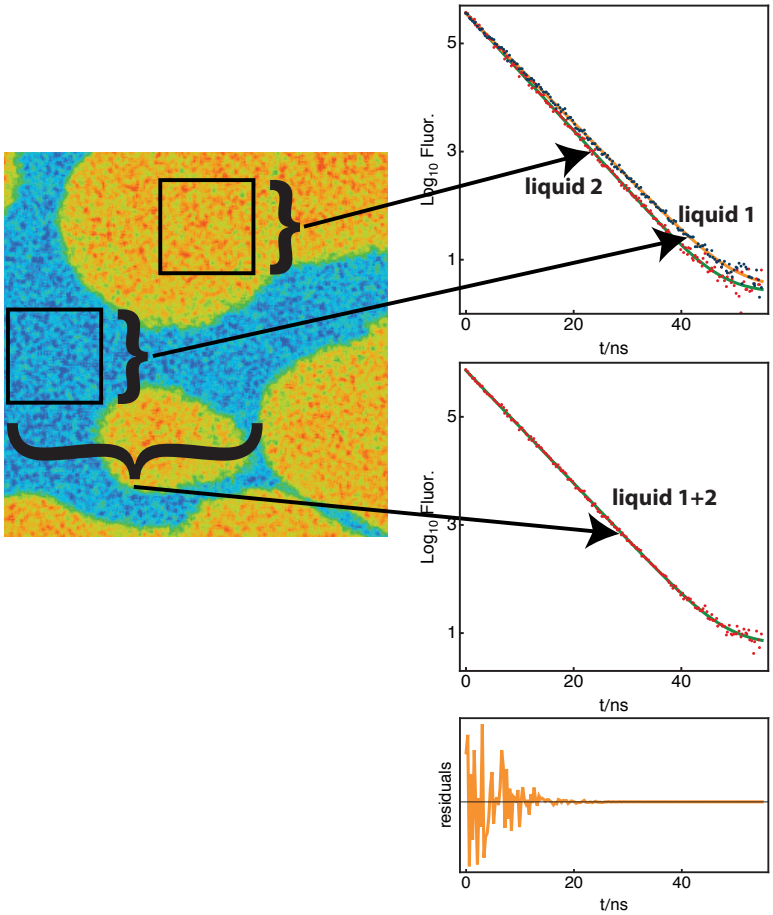

FIG. 5. FLIM measurements can resolve very similar decay times unresolvable by bulk measurements. (**left**) A typical FLIM image taken during NG-type transformation in TPP from liquid 1 to liquid 2. (**top right**) Two simulated exponential decays with decay times of 4.0 and 4.3 ns. (**bottom right**) The sum of the two traces shown above and a fit to a single exponential decay function.

Additional data

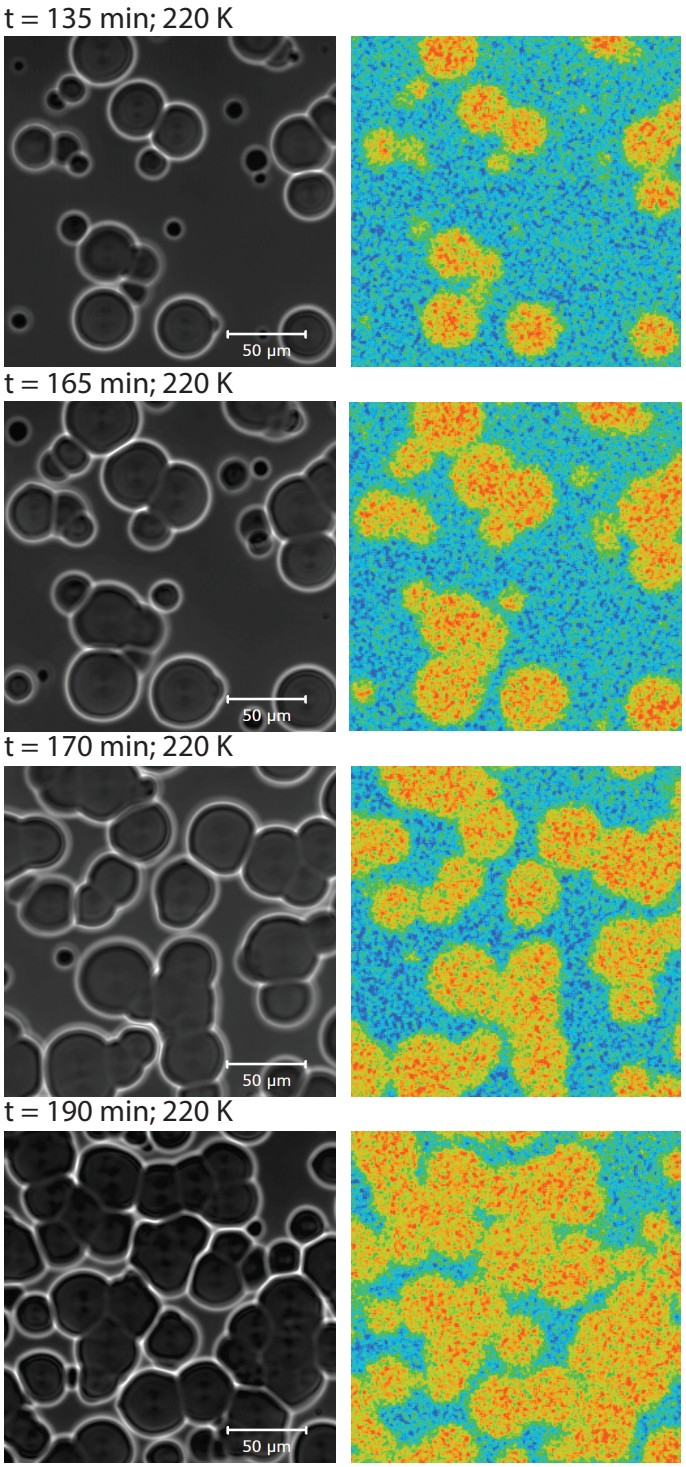

FIG. 6. Representative images of typical patterns associated with the LLT in TPP. The images in the left hand side panels were obtained using phase-contrast microscopy while the images on the right were obtained using FLIM using the dye coumarin 153 (C153). These images were obtained by quenching to 220 K for the indicated amount of time (nucleation and growth, FLIM scaling 4.21 ns (red) to 4.46 ns (blue)).

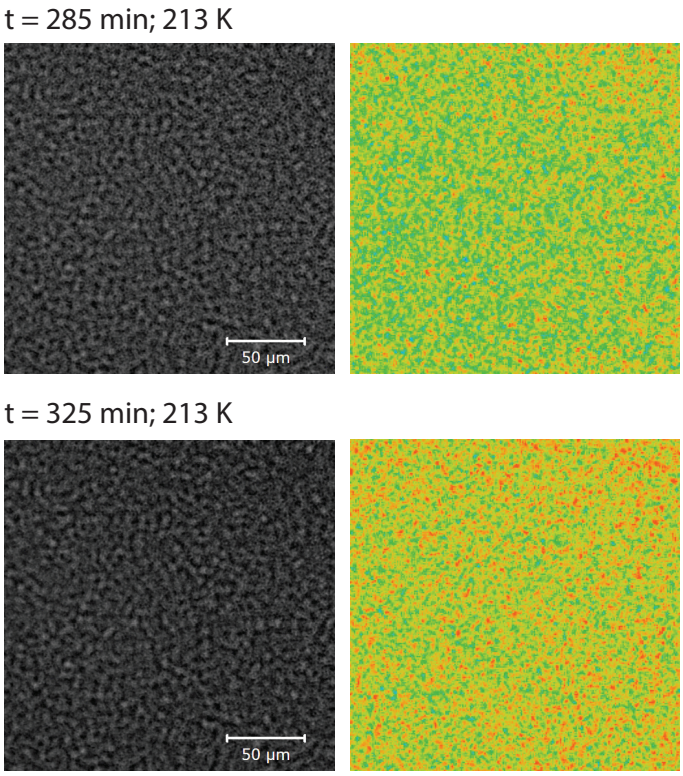

FIG. 7. As FIG. 6. These images were obtained by quenching to 213K for the indicated amount of time (spinodal decomposition, FLIM scaling identical to FIG. 6).

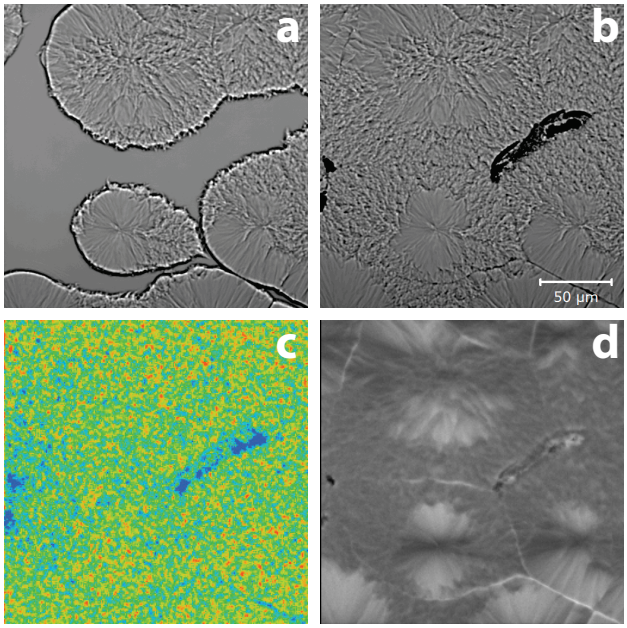

FIG. 8. Formation of a second crystalline phase in TPP quenched to 226 K. (**a**) DIC image halfway through the NG-type transformation from liquid 1 to liquid 2. Inside the liquid 2 droplets crystalline features appear. (**b**) As in (a) but at the end of the LLT transformation. (**c**) FLIM map of the same area as in (b) using fluorescence from C153 (FLIM scaling 4.1 (red) to 4.3 ns (blue)). (**d**) Fluorescence intensity (scaling grey ~2,500/pixel, white ~3,300/pixel).

References

1. Horng, M.; Gardecki, J.; Papazyan, A.; Maroncelli, M. Subpicosecond Measurements of Polar Solvation Dynamics: Coumarin 153 Revisited. *J Phys Chem* **1995,** *99*, 17311-17337.
2. Maroncelli, M. Continuum estimates of rotational dielectric friction and polar solvation. *J Chem Phys* **1997,** *106*, 1545-1555.
3. Shirota, H.; Castner, E. Solvation in highly nonideal solutions: A study of aqueous 1-propanol using the coumarin 153 probe. *J Chem Phys* **2000,** *112*, 2367-2376.
4. Maroncelli, M.; Zhang, X.-X.; Liang, M.; Roy, D.; Ernsting, N. P. Measurements of the complete solvation response of coumarin 153 in ionic liquids and the accuracy of simple dielectric continuum predictions. *Faraday Discuss.* **2011,** *154*, 409-424.
5. Funston, A. M.; Fadeeva, T. A.; Wishart, J. F.; Castner, E. W. Fluorescence probing of temperature-dependent dynamics and friction in ionic liquid local environments. *J Phys Chem B* **2007,** *111*, 4963-4977.
6. Zhao, X.; Kivelson, D. Light-Scattering Studies of Simple Molecular Supercooled Liquids: Structural Considerations. *J Phys Chem* **1995,** *99*, 6721-6732.
7. Van Der Zwan, G.; Hynes, J. T. Time-Dependent Fluorescence Solvent Shifts, Dielectric Friction, and Nonequilibrium Solvation in Polar Solvents. *J Phys Chem* **1985,** *89*, 4181-4188.
8. Wynne, K.; Hochstrasser, R. Coherence and adiabaticity in ultrafast electron transfer**1999,** *107*, 263-309.
9. Böttcher, C. J. F. *Theory of Electric Polarization*. Elsevier: Amsterdam, 1973.
10. Cave, R. J.; Castner, E. W. Time-Dependent Density Functional Theory Investigation of the Ground and Excited Statesof Coumarins 102, 152, 153, and 343. *J Phys Chem A* **2002,** *106*, 12117-12123.
11. Murata, K.-I.; Kurita, R.; Tanaka, H.; Tokuyama, M.; Oppenheim, I.; Nishiyama, H. Dynamic Nature of the Liquid-Liquid Transition of Triphenyl Phosphite Studied by Simultaneous Measurements of Dielectric and Morphological Evolution. In *COMPLEX SYSTEMS: 5th International Workshop on Complex Systems*, AIP: 2008; Vol. 982, pp 196-198.
12. Lewis, J. E.; Maroncelli, M. On the (uninteresting) dependence of the absorption and emission transition moments of coumarin 153 on solvent. *Chem Phys Lett* **1998,** *282*, 197-203.
13. Jortner, J.; Bixon, M. Intramolecular vibrational excitations accompanying solvent-controlled electron-transfer reactions. *J Chem Phys* **1988,** *88*, 167-170.
14. Dobek, K. The influence of temperature on Coumarin 153 fluorescence kinetics. *J Fluoresc* **2011,** *21*, 1547-1557.
15. Dobek, K.; Karolczak, J. The influence of temperature on C153 steady-state absorption and fluorescence kinetics in hydrogen bonding solvents.**2012,** *22*, 1647-1657.